

1 **Hydro-climatic variation drives the long-term ecological evolution of neotropical**
2 **floodplain lakes: an example from the Magdalena River system, Colombia**

3 **Authors:** Laura Lopera-Congote¹, Jorge Salgado^{1,2,3*}, María Isabel Vélez⁴, Andrés Link⁵,
4 Catalina González-Arango¹

5 1. Laboratorio de Palinología y Paleoecología Tropical, Universidad de los Andes, Bogotá,
6 Colombia

7 2. Facultad de Ingeniería, Universidad Católica de Colombia, Bogotá, Colombia

8 3. School of Geography, Nottingham University, Nottingham, UK

9 4. Department of Geology, University of Regina, Regina SK, Canada

10 5. Laboratorio de Ecología de Bosques Tropicales y Primatología, Departamento de
11 Ciencias Biológicas, Universidad de Los Andes, Bogotá, Colombia

12 **Key words:** Climate change, Diatoms, Floodplains, hydrological connectivity,
13 Paleolimnology, Tropical Rivers

14 *Corresponding author: Jorge Salgado, Sir Clive Granger Building, Nottingham, NG7 2RD,
15 UK ; Email: Jorge.SalgadoBonnet@nottingham.ac.uk

16 **Abstract**

17 The Magdalena River in Colombia and its floodplain lakes are key ecosystems for the subsistence
18 of Colombian society. Yet, hydrologic regulation, pollution, deforestation and climate change are
19 threatening its ecological integrity. To understand how these floodplain lakes respond over
20 decadal-centennial scales to natural and anthropogenic stressors, we selected two shallow lakes
21 with varying degree of connectivity to the River and assessed their historical ecological and
22 limnological change through a multi-proxy analysis of diatoms, geochemistry and lake's
23 morphometric variation resulting from extreme periods of high floods and droughts. The
24 reconstruction of the more isolated San Juana Lake covered the last c.500 years. It showed
25 riverine-flooded conditions from c.1555-1741 characterised by high detrital inputs, reductive
26 conditions, and dominance of planktonic diatoms. From c.1758-1954, the riverine meander
27 became disconnected, conveying into a marsh-like environment rich in aerophil diatoms and
28 organic matter. The current lake was then formed around the mid 1960s and a diverse lake-
29 associated diatom flora developed. Lake waters became more oxygenated, while sedimentation
30 and nutrients increased through time since the lake formation. The reconstruction for Barbacoas
31 Lake, a waterbody directly connected to the Magdalena River, spanned the last 60 years and
32 showed alternating riverine-wetland-lake conditions dominated by planktonic and benthic diatoms
33 respectively. An exception was however observed, during a prolonged period of low rainfall
34 between 1989-1992, where the lake almost desiccated and where aerophil diatoms prevailed.
35 Inferences of flood magnitudes and river connectivity in the lakes were supported by parallel
36 increases in Zr/Fe (flooding) and detrital inputs (Ti/Ca) along with decreases in sedimentary OM.
37 We proposed that lake hydrological connectivity to the Magdalena River is a main factor
38 controlling lake long-term responses to human pressures. Highly connected lakes may respond

39 more acutely to ENSO events while isolated lakes might be more sensitive to local land-use
40 changes.

41 1. INTRODUCTION

42 Tropical floodplain lakes are subject to natural hydrological dynamics imposed by the
43 river, and thus are exposed to natural extreme climate events such as floods and droughts
44 (Death, 2010; Poff & Ward, 1989; Resh et al., 1988). These are known to influence primary
45 productivity, community assembly (Junk, Bayley, & Sparks, 1989), increase or interruption
46 of physical ecological connectivity (Amoros & Bornette, 2002), which in turn impacts
47 habitat quality (Lake, 2000). However, natural hydrological dynamics of tropical
48 floodplains can be affected by long-term (decades-centuries) human-derived
49 modifications such as river damming, deforestation, land use change and climate change
50 (Salgado et al., 2020; Van Looy et al., 2019; Angarita et al., 2017).

51 The Magdalena River in Colombia is one of the largest rivers (1540 km) of South America
52 (Best, 2019) discharging over 7.100 m³/s into the Caribbean Sea (Figure 1). It dissects the
53 country from South to North, as it runs between the Central and Eastern Andean
54 Cordilleras. The river contains the largest floodplain areas of the country (320.000 Ha,
55 67%; Montoya-Moreno & Aguirre, 2009), hosting over 70% of the nation population and
56 Gross Domestic Product- GDP (Mojica et al., 2006). Local human communities also
57 depend on this riverine ecosystem as it contains one of the largest fish provisions in the
58 region, with key economic species such as the Magdalena catfish (*Pseudoplatystoma*
59 *magdaleniatum*) or the Bocachico (*Prochilodus magdalenae*) (Caballero et al., 2001). Its
60 floodplains, lakes, wetlands and primary riparian forests are considered a biodiversity
61 hotspot home to endemic birds such as the Critically Endangered blue-billed curassow

62 (*Crax alberti*) and other migratory bird species such as the fishing eagle (*Pandion*
63 *haliaetus*), the Yellow-billed Cuckoo (*Coccyzus americanus*) and the Eastern Kingbird
64 (*Tyrannus tyrannus*) (Angel-Escobar et al., 2014). Other endangered and charismatic
65 vertebrates found in the region, include the brown spider monkeys (*Ateles hybridus*), the
66 American manatee (*Trichechus manatus*), the lowland tapir (*Tapirus terrestris*) and the
67 river otter (*Lontra longicauda*) (Angel-Escobar et al., 2014).

68 Deforestation in the Magdalena River basin has been steadily increasing over the last six
69 decades, with current rates being three-fold higher than those from the 1950s (Ayram et
70 al., 2020; Restrepo et al., 2018; Etter et al., 2008). This profound transformation of the
71 landscape has come with a great environmental burden as the river and associated lakes
72 have experienced excess in sediment yields, water pollution, habitat fragmentation, and
73 freshwater fish population declines (Best, 2019; Restrepo et al., 2018; Restrepo, 2015). In
74 addition, more than 20 large dam projects (> 20 MW hydropower capacity) across the
75 Magdalena River and tributaries have been constructed or are on their way of
76 implementation resulting in higher fish extinction risks and severe river flow reduction
77 (Angarita et al., 2019; Carvajal-Quintero et al., 2017).

78 The growing interplay between human-caused stressors in the Magdalena river is
79 therefore, bringing new challenges to the management and conservation of these tropical
80 riverine ecosystems, highlighting the need for a better understanding of the historical
81 trajectory of change in response to natural causes and to our past and present actions to
82 promote adaptive management approaches (Van Looy et al., 2019). However, limnological

83 instrumental records for floodplain lakes are mostly inexistent in the catchment area of
84 the river. The study of lake sediments through the use of palaeoecological techniques
85 have shown to provide continuous data on sedimentological changes and aquatic
86 communities over time allowing to track back in time the effects of land use change and
87 its hydrological and limnological effects (Zeng et al., 2018; Salgado et al., 2020).

88 By focusing on two floodplain lakes (Barbacoas and San Juana) that differ in degree of
89 hydrological connectivity to the Magdalena River and that have been subjected to
90 frequent changes in land use over the last decades, this study aims to provide information
91 on the long-term ecological responses of these systems to both natural hydrological and
92 human-induced stressors. In particular we wanted to respond the following questions: (1)
93 how have the San Juana and Barbacoas lakes evolved over time in response to natural and
94 human-induced factors? And (2) how does the varying degree of hydrological connectivity
95 to the Magdalena River affect the dynamics and stability of these ecosystems?

96 We hypothesize that the more connected ecosystem (Barbacoas) would have been more
97 dependent on the hydrological dynamics imposed by the Magdalena River, and that the
98 more isolated ecosystem (San Juana), would have been more dependent of changes in the
99 local environment (Salgado et al., 2019; Swan & Brown, 2011). We used a multi-proxy
100 analysis (fossil diatom, organic matter content, and sediment geochemistry) on sediment
101 cores taken at each lake to reconstruct environmental and ecosystem change over the last
102 few centuries.

103 2. METHODS

104 **2.1 Study Area**

105 Barbacoas Lake (6°44'26''N 74°14'36''W) is located on the western margin of the
106 Magdalena River, and is directly connected to it via the Barbacoas creek, which has an
107 approximate length of 6.3 km long (Figure 1). Barbacoas is a shallow lake (average depth=
108 1.2 meters) with a superficial area of 10 km², brown-stained waters (mean secchi depth=
109 0.39 ±0.47 cm), pH of 7.25 ±0.26 and mean daily surface water temperature of 33.7
110 ±0.35°C (Table 1). San Juana Lake is located (6°38'32''N 74°09'24''W) on the eastern
111 margin of the Magdalena River (Figure 1). It has a superficial area of 1.05 km² and is
112 characterised by average water depths of 2.2 meters, brown-stained waters (mean secchi
113 depth= 53 ±0.55 cm), and a mean daily surface temperature of 30.15 ±0.93 °C (Table 1).
114 The lake is fed by the San Juan River on the south that outflows on the west joining later
115 the Carare River before spilling into the Magdalena River near the town of Bocas del
116 Carare (6°46'48''N 74°06'14''W). The hydrological river distance between the Magdalena
117 and the San Juana Lake is approximately of 18.5 km.

118 **2.2 Core sampling**

119 In an attempt to collect information from both river-borne and in-lake processes we
120 retrieved single-short sediment cores from semi-littoral areas near the mouth of the
121 outflow of each lake using a wide-bore (diameter of 10 cm) corer (Aquatic Instruments
122 inc.). The core from the San Juana Lake (LSAN-1) was collected at a water depth of 100 cm
123 (6°38'32''N 74°09'24''W). The core from Barbacoas Lake (LBARB-1) was retrieved at a
124 water depth of 90 cm (6°44'26''N 74°14'36''W). Each core was subsampled in the field at 1

125 cm intervals; changes in lithostratigraphy were recorded prior to extrusion. The sediments
126 were then kept refrigerated at the Tropical Palynology and Paleoecology Laboratory,
127 Universidad de Los Andes for further analyses.

128 **2.3 Dating and age-depth model**

129 The L-SAN1 and LBARB-1 cores were dated using radionuclide measurements of ^{210}Pb ,
130 ^{226}Ra , ^{137}Cs and ^{241}Am by direct gamma assay (Appleby et al., 2001) in the Environmental
131 Radiometric Facility at University College London, UK. For LSAN-1 the top 20 cm of the
132 core were dated and the age of the remaining core sediment samples (20-50 cm) were
133 extrapolated following Zeng et al., (2018) by using linear regression analysis according to
134 the four older dated sediment samples, i.e. 14.5 cm, 15.5 cm, 17.5 and 18.5 cm. For
135 LBARB-1, the sediment samples were dated every three centimetres, along the core.

136 **2.4 Geochemical analysis**

137 The organic matter (OM) content of each core was measured using the method of loss-on-
138 ignition (LOI; Dean 1974). Sampling resolution for LSAN-1 core was at 1 cm for the top 20
139 cm samples, and at every 2 cm for the remaining 30 cm of the core samples. For LBARB-1
140 core, sampling resolution was at 1 cm throughout the core. Shifts in OM content were
141 used as a proxy of flooding (river influence) following Schillereff et al., (2014). During high
142 floods OM is expected to decline through dilution from a greater deposition of terrigenous
143 sediments associated with the river flow (Rapuc et al., 2019). In turn, OM is expected to
144 increase during dry periods through increased in-lake primary production and decreased
145 allochthonous input (Schillereff et al., 2014).

146 Sediment geochemistry was measured using X-ray fluorescence (XRF) with an Xmet 7500
147 portable analyser spectrometer (Oxford instruments Inc.). Around 3 grams of dry
148 sediment, 1 cm thick sample was analysed for XRF. A sampling resolution of every 1 cm
149 was used for the top 18 cm sediment samples in both cores, and of every 3 cm for the
150 remaining bottom samples of both cores. We obtained two XRF readings (1 minute of
151 length) for each sediment sample and the median value of both readings was used for
152 statistical analysis. The XRF portable analyser spectrometer was calibrated against
153 certified material prior to analysis (Conrey et al., 2014) and all XRF measurements were
154 run using the Mining method, which detects elements occurring in very low (<0.01 ppm)
155 concentrations (Gasdia-Cochrane, 2017). A total of 31 samples for LSAN-1 and of 29
156 samples for LBARB-1 were analysed for phosphorus (P), iron (Fe), manganese (Mn),
157 titanium (Ti), calcium (Ca), and zirconium (Zr). The ratios of these elements (excluding P)
158 were used as proxies for river-borne and in-lake processes as follow: flooding Zr/Fe
159 (Schillereff et al., 2014; Davies et al., 2015), detrital input Ti/Ca (Salgado et al. 2020; Davies
160 et al., 2015), and oxygenation of the water column Mn/Fe (Davies et al., 2015). Generally
161 rivers during low flow periods deliver comparatively less sediments to lakes, and these are
162 normally fine-grained silts; during slightly elevated flows, clays and Fe commonly occur
163 (Schillereff et al., 2014). During peaks of high floods, coarse-grained (Zr) sediments are
164 expected to increase (Schillereff et al., 2014). Ti is an unambiguous indicator of
165 allochthonous coarser inputs from the catchment (Cohen, 2003), while Ca is often
166 associated with in-lake production (Tjallingii et al., 2007). As such, higher values of Ti/Ca
167 ratio may indicate greater detrital input (Salgado et al., 2020). Iron (Fe) and manganese

168 (Mn) provide information about changing redox conditions (Davies, 2015). In a reducing
169 (low oxygen) environment, the solubility of Fe and Mn increases, being Mn more readily
170 affected (Boyle, 2002). An increase in Mn/Fe ratio can thus indicate the onset of aerobic
171 conditions. As so, greater river influences into the lakes were inferred by increases in
172 flooding, sedimentation rates, detrital inputs and concomitant reductions in OM.

173 **2.5 Diatoms**

174 Approximately 0.3 gr of dry sediment per sample were used for diatom analyses following
175 Battarbee (1986). Each sample was placed in a beaker with 30 mL of hydrogen peroxide
176 (10%) for approximately 24 hours, or until the reaction stopped. After, 100 mL of distilled
177 water was added to each of the samples and they were left until the water column was
178 clear. Then, 0.6 mL of each sample was placed on a microscope slide and allowed to dry
179 after which it was mounted using Naphrax and then 400 diatoms were counted and
180 classified. For LSAN-1 core sampling resolution was every 1 cm in the top 20 cm, and every
181 4 cm for the remaining of the core, for a total of 27 samples. For LBARB-1 core, we used a
182 sampling resolution of 2 cm throughout the core, for a total of 22 samples. The differential
183 lake sampling resolution was due to the differences in sedimentation rates and the
184 temporal resolution we wanted to achieve for the recent decades. The diatom species
185 were identified using (Lange-Bertalot & Meltzlin, 2007; Kramer & Lange-Bertalot, 1986,
186 1991a, 1991b; Diatoms of North America database; diatoms.org) and then grouped into
187 the following functional groups according to their ecological preference: Aerophil, Benthic
188 and Planktonic (Table 2). For the Benthic category ecological preferences related to

189 productive and acidic/dystrophic waters were also included (Viktória et al., 2017). Species
190 of the genus *Eunotia*, *Pinnularia*, *Nitzschia*, *Encyonema* and *Gomphonema* had very low
191 counts and therefore they were aggregated into a single category according to their
192 respective genus.

193 **2.6 Data Analysis**

194 Statistical analyses were performed following four logical steps:

195 2.6.1 Changes in diatom assemblages

196 To detect major zones of temporal diatom change, and assess main compositional
197 changes, we used a combination of stratigraphically Constrained Hierarchical Clustering
198 (Coniss) analysis and Rank Clocks Analyses (RCA; Collins et al., 2008). Coniss analysis was
199 performed using the *Rioja* package in R (Juggins & Juggins, 2019). RCAs were performed
200 with the *Codyn* package in R (Hallet et al., 2016). RCA identifies which species show the
201 greatest change in abundance at each temporal zone revealed by clustering analysis on a
202 clock-like diagram, where 12 o'clock on the vertical axis is the starting point of the data
203 (Collins et al., 2000). Prior to Coniss and RCA analyses, diatom counts were square root
204 transformed in order to weight the varying relative abundances of the different diatom
205 species (Okansen et al., 2010).

206 2.6.2 Changes in sediment geochemistry

207 Temporal trends of change in the selected geochemical indices (detrital inputs, erosion,
208 flooding, and oxygenation of the water column) were modelled using Generalised Additive

209 Models (GAM) on the *mcgv* package in R (Wood & Wood, 2015). GAMs were run using the
210 default settings on each geochemical index ratio as the response variable and core depth
211 as the predictor variable using the method “REML”.

212 2.6.3 Trajectories of ecological and geochemical change

213 The main trajectories of ecological and geochemical change over time for each lake were
214 then assessed using Multiple factor analysis–MFA (Pagès, 2002). MFA allows incorporating
215 simultaneously the amount of variation explained by the different diatom functional
216 groups and geochemical index ratios, while visually assessing trends in trajectory of
217 change in the multidimensional space. We standardised the diatom, LOI, sedimentation
218 rates and geochemical index ratios by applying a weight equal to the inverse of the first
219 eigenvalue of the analysis of the group (Pagès, 2002). The MFAs were performed in R
220 using the package *FactoMineR* (Pagès, 2002).

221 2.6.4 Hydro-climatic variation and lake responses

222 To quantify how lakes have responded to extreme long-term climatic events (ENSO) we
223 run a Standardised Precipitation-Evapotranspiration Index–SPEI analysis (Vicente-Serrano
224 et al., 2010). This analysis uses historical climatic data to generate a drought index based
225 on the difference between precipitation and potential evapotranspiration across a given
226 area, allowing the identification of years with extreme drought or excess water (Vicente-
227 Serrano et al., 2010). The SPEI index data were downloaded from
228 <https://spei.csic.es/map/maps.html#months=1#month=3#year=2020> for the interval
229 [between 1985 and 2016](#). Years with severe drought or excess precipitation were obtained

230 using the annual mean data (i.e. 12-month time scale). The Global SPEI database is fed by
231 worldwide monthly drought conditions data with a spatial resolution is of 0.5 degrees
232 (Vicente-Serrano et al., 2010).

233 Years with SPEI index values between -0.5 and 0.5 are considered to fall within a normal
234 climatic variability (Vicente-Serrano et al., 2010), whereas years with values < -2 are
235 considered as extremely wet, and values > 2 are considered as extremely dry (Vicente-
236 Serrano et al., 2010). Extreme wet and dry years were thus identified for our study area
237 and then, the total surface area of each lakes was measured during these extreme events.
238 To calculate the total surface area of each lake at a given time-period we used a
239 supervised image classification analysis in Qgis desktop 3.10.5. The SPEI index data was
240 further correlated against the geochemical index Zr/Fe to test the feasibility of this ratio as
241 a reliable proxy for river influence (flooding). Correlation patterns and significance
242 between ZR/Fe and SPEI index data were again achieved via GAM using the above
243 mentioned protocols for the geochemical indices.

244 **1. RESULTS**

245 **3.1 Age model and sedimentation rates**

246 The LSAN-1 core was of 50 cm long with ^{137}Cs and ^{241}Am activities indicating the 1963
247 maximum fallout of the atmospheric nuclear bomb around the top 19 cm section (Figure
248 S1a). The resulting ^{210}Pb dating model indicates that the top 20 cm spanned the last c. 120
249 years with the extrapolating ^{210}Pb dates bellow this core depth suggesting a sediment
250 record covering approximately the last 500 years (Figure 2a). Sedimentation rates within

251 the ^{210}Pb dated portion of the core (top 19 cm) gradually increased from $0.024 \text{ g cm}^{-2} \text{ yr}^{-1}$
252 at 18 cm to $0.49 \text{ g cm}^{-2} \text{ yr}^{-1}$ at the top of the core with two marked peaks of $0.12 \text{ g cm}^{-2} \text{ yr}^{-1}$
253 and $0.23 \text{ g cm}^{-2} \text{ yr}^{-1}$ corresponding at around the years 1930 and 1990 respectively.

254 The LBARB-1 core was 40 cm long with ^{137}Cs activity showing a peak at 36.5 cm indicating
255 the maximum fallout level in 1963 (Figure S1b). Since the CRS model placed 1963 at a
256 shallower depth (29.5 cm), the chronology was corrected by placing the year 1963 at a
257 depth of 36.5 cm (Figure S1b). The resulting ^{210}Pb dating model spanned therefore the last
258 c. 60 years; i.e. 2016- 1959 (Figure 2b). Sedimentation rates were generally high across the
259 sediment record, ranging between $0.3 \text{ g cm}^{-2} \text{ yr}^{-1}$ at 30 cm to $3 \text{ g cm}^{-2} \text{ yr}^{-1}$ at 6 cm (2016-
260 2014). Very low ^{210}Pb activities within the top first centimetres of the core indicates
261 possible sediment mixing, and thus the top 3.5 cm sediments were assumed to be formed
262 within the same year.

263 **3.2 Diatom community change**

264 *San Juana Lake*

265 A total of 19 diatom taxa were found in LSAN-1 (Figure 3). Clustering analysis and RCA
266 revealed the following major zones of change in the diatom assemblages:

267 *Zone 1 (48.5-36.5 cm; c. 1555-1747 CE)*

268 This zone was characterised by dominance of *Aulacoseira ambigua* (Figure 3). The diatoms
269 *Pinnularia* spp. *A. granulata*, *Neidium saccoense*, *Capartogramma crucicola*, and *Caloneis*
270 *amphisbaena* also occurred but with lower abundances.

271 Zone 2 (35.5-12.5 cm; c. 1758-1965 CE)

272 This zone was characterised by a co-dominance of *Pinnularia* spp., *A. granulata*, and *A.*
273 *alpigena* (Figure 3). The species *Diadesmis confervacea* and *Staurosirella pinnata* were
274 also present in low abundances.

275 Zone 3 (22.5-0.5 cm; c. 1967-2016 CE)

276 This zone was dominated by *Pinnularia* spp., and *A. granulata* (Figure 3). The diatom
277 species *A. alpigena* was present but with lower abundances compared to the previous
278 zone. *D. confervacea*, *Eunotia* spp., and *Sellaphora alastos* increased while other diatoms
279 present, but in lower abundances included *Stauroneis neohyalina*, *Gomphoneis erienne*
280 and *Encyonema minutum* var. *pseudogracilis*.

281 *Barbacoas Lake*

282 A total of 21 diatom taxa were found in LBARB-1 core (Figure 4). Clustering analysis and
283 RCA indicated three main temporal zones of diatom assemblage change:

284 Zone 1 (38.5-24.5 cm; c. 1959-1984 CE)

285 In this zone *A. granulata*, *Aulacoseira* sp., *A. alpigena* and *Actinella disjuncta* dominated
286 the assemblages (Figure 4). In minor proportions and mainly restricted to this zone were
287 *A. distans* and *D. confervacea*. *A. herzogii* peaked around 22 cm. Other taxa occurring
288 with lower abundances included *Eunotia* spp., *Pinnularia* spp., and *Cyclotella*
289 *meneghiniana*.

290 Zone 2 (29-22 cm; c. 1989-1992 CE)

291 During this time *A. granulata*, *A. granulata var. angustissima*, *Aulacoseira sp.*, *A. alpigena*
292 and *D. confervacea* dominated (Figure 4). It is important to notice that between 21-22 cm
293 (1989 and 1992 respectively) species such as *A. herzogii* and *C. menenghiana* disappeared
294 from the fossil record but reappeared post-1992. Also, *Luticola mutica* appeared around
295 22 cm (1989) peaking around 21 cm (1992). *Pinnularia spp.*, *Encyonema spp.*, and *Eunotia*
296 spp., were present in lower proportions and remained constant through this interval.

297 Zone 3 (21-0 cm; c. 1989-1992 CE)

298 This zone was marked by dominance of *A. granulata var. angustissima* along with
299 increases in *A. herzogii*, *Frustulia crassinerva*, and *Pinnularia spp.*, (Figure 4). At the core
300 depths 15 cm and 5 cm (2011 and 2015 respectively), all diatoms disappeared from the
301 fossil record.

302 3.3 SPEI Analysis

303 The SPEI analysis (Figure S2) identified extreme dry periods during 1992, 1997, 1998 and
304 2015 and extremely wet periods in 1951, 1999, and 2011. Accordingly, each lake surface
305 area was calculated for regular years when there were no extreme events (1985 and
306 2016), for an extreme El Niño draught in 1992, and for an extreme wet La Niña event in
307 2011 (Figure 5). Calculated lake surface area values for the San Jana Lake were of 0.64 Km²
308 in 1985, of 0.56 Km² in 1992, of 0.59 Km² in 2011 and of 0.52 Km² in 2016 (Figure 5a).

309 Lake surface area for Barbacoas Lake was of 8.7 Km² in 1985), of 2.8 Km² in 1992, of 2011
310 8.4 Km² in 2011 and of 10.37 Km² in 2016 (Figure 5b).

311 **3.4 Geochemical analysis**

312 *San Juana Lake*

313 The GAM on LOI explained a significant ($p < 0.001$) 96.8% of the temporal variation in OM
314 content (Figure 6a). The analysis revealed that OM was relatively low (10%-18%) between
315 50 and 22 cm (c. 1531-1867 CE). A subsequent increase (28-29%) in OM was observed
316 within the upper 21 cm of the core (c. 1879-2016 CE). The analysis further explained a
317 significant ($p > 0.002$) 37.5% of the temporal variation in Mn/Fe (oxygenation of the water
318 column) with values increasing gradually over time (0.0021 to 0.005) and being more
319 pronounced from 21 cm upwards. The GAM models for the ratios Ti/Ca (detrital inputs)
320 and Zr/Fe (flooding) explained a significant ($p < 0.001$ in both cases) 82% and 50% of the
321 total temporal variation respectively. Both indices gradually declined (1.30 to 0.98 and
322 0.033 to 0.016 respectively) within the top 21 cm of the core. The GAM model for P
323 concentrations in the lake sediments, also explained a significant ($p = 0.02$) 16.5% of the
324 temporal variation showing a gradual increase (0.12 to 0.18) over time that became more
325 pronounced since 1967.

326 *Barbacoas Lake*

327 The GAM on LOI explained a significant ($p < 0.001$) 88% of the temporal variation in OM
328 content (Figure 6b). The analysis revealed that between 40-30 cm, OM content was

329 relatively high, ranging between 20%-30%. A marked subsequent decrease in OM was
330 observed within the top 29 cm of the core (c. 1981-2016 CE) reaching values of 5-6%
331 towards recent times. The analysis for the Mn/Fe ratio explained a significant ($p > 0.001$)
332 53% of the temporal variation showing a marked increase in ratio values (0.00092 to
333 0.0012) since around the 25 cm sample. GAM on the Ti/Ca ratio also explained a
334 significant ($p < 0.001$) 62% of the temporal variation showing a gradual increase (0.5 to 0.8)
335 within the top 30 cm of the core from values. The analysis for Zr/Fe ratio explained a
336 significant ($p < 0.001$) 77% of the total temporal variation. Zr/Fe values were relatively low
337 (0.0001) between 40-30 cm (c. 1959-1975 CE) with a subsequent increase (0.0003)
338 between 26 cm and 8 cm (c. 1983-2013 CE) and a subsequent reduction (0.00025) in Zr/Fe
339 from 7-0 cm (c. 2014-2016 CE).

340 The GAM analysis for the SPEI data and the flooding proxy (Zr/Fe ratio) explained a
341 significant ($p = 0.003$) 60% of the temporal variation in the San Juana Lake and a significant
342 ($p = 0.001$) 36% in Barbacoas Lake (Figure 5c). The analysis revealed a negative correlation
343 between SPEI and flooding. Wet years ($\text{SPEI} > 0$) were correlated with low Zr/Fe ratios and
344 dry years ($\text{SPEI} < 0$) with higher Zr/Fe ratio values.

345 **3.5 Shifts and rates of diatom community and environmental change**

346 The MFA for San Juana Lake showed that Dimension 1 (D1) explained 31.5% of the total
347 diatom and geochemical variation, whereas dimension 2 (D2) explained 17.5% (Figure 7a).
348 The group categories contributing the most to D1 included acidic/dystrophic diatoms
349 (27%), geochemical processes (24%) and benthic/productive diatom species (22%).

350 Planktonic (48%) and aerophil diatoms (30%) explained most of the variation of D2. Three
351 different temporal categories were distinguished in the ordination plot. Historical times (c.
352 1500s-1750 CE) were placed on the left hand side of the diagram and were characterised
353 by high flooding, low OM content, and low sedimentation rates. The planktonic diatom *A.*
354 *ambigua* and the acidic/dystrophic *Pinnularia* spp., *C. amphisbaena*, *C. crucicola*, and *N.*
355 *sacoense* dominated during this early category. The second category (c. 1783-1954 CE)
356 was placed on the top centre of the diagram with the planktonics *A. alpigena*, and *A.*
357 *granulata* and the aerophil *S. pinnata* dominating the assemblages. Samples moved then
358 towards the right hand side of the multivariate diagram forming the third group (1961-
359 2016 CE; Figure 6a). This group was characterised by low flooding, greater OM content
360 and high sedimentation rates. Diatom species occurring in this group included the aerophil
361 *D. confervacea*, the benthic/productive *Nitzschia* spp., *G. eriense*, and *C. cuspidata*, and
362 the acidic/dystrophic, *Eunotia* spp., *S. alastos*, and *S. supergracilis*.

363 The MFA for Barbacoas Lake showed that D1 explained 19.6% of the total diatom and
364 geochemical variation, while D2, explained 15.8% (Figure 7b). The diatom functional
365 groups contributing the most to D1 variation were planktonic (29%) and
366 benthic/productive diatoms (24%), whilst geochemical proxies accounted for 22%. The
367 diatom functional groups contributing the most to D2 were acidic/dystrophic (32%),
368 planktonic (24%) and aerophil (22%) diatoms. Three temporal categories were
369 distinguished in the ordination plot. Historical times (1980-1960) were placed on the right
370 hand side of the plot and characterised by small flooding events, low sedimentation and
371 high OM content (Figure 7b). Diatom species within this historical cluster included the

372 planktonic *A. distans*, *Fragilaria* spp., and *A. alpigena*, the benthic/productive *A. disjuncta*
373 and *H. elongata* and the acidic *Eunotia* spp. The second association included the years
374 1985, 1986, 1999, 2012, and 2014 and was placed on the left-down side of the diagram.
375 Oxygenated water column conditions prevailed during these years along with a
376 dominance of the aerophil *L. mutica* and the planktonic *A. granulata* var. *angustissima*. The
377 third temporal category included the years 1989, 1992, 2003, 2006, 2010 and 2015 was
378 placed on the centre of the plot. This temporal association was characterised by high
379 detrital inputs, high flooding and high sedimentation rates along with a prevalence of the
380 planktonic *A. herzogii*, the benthic/productive *Nitzschia* spp. and *Gomphonema* spp., and the
381 acidic/dystrophic *Encyonema* spp., *Stauroneis* spp., *F. crassinervia*.

382 4. DISCUSSION

383 Tropical floodplain ecosystems are rapidly deteriorating across the globe due to multiple
384 stressors including changing hydrology, climate and human disturbance (Tockner et al.,
385 2010). Yet little is known, in particular in the neotropics, about how these valuable
386 ecosystems are responding on a long-term (decades-centuries) scale to these stressors. As
387 we discuss bellow, the palaeolimnological multi-proxy approach on Barbacoas and San
388 Juana Lakes used in this study provides a first approximation on how neotropical lowland
389 floodplain lakes may respond through time according to variable degrees of connectivity
390 to the main river and human induced stressors.

391 4.1 Long-term evolution of lakes and their response to extreme events

392 *San Juana Lake*

393 Over the last c. 500 years San Juana Lake transitioned from a river-governed system, to a
394 wetland, and eventually to the lake it is today, probably as a consequence of a progressive
395 disconnection to the Carare River, tributary of the Magdalena River. This is interpreted
396 from the dominance in planktonic species such as *A. ambigua* and *A. granulata*, and *C.*
397 *amphisbaena* around c.1555-1747 CE (Zone 1) that reflect water mixing and river
398 influence (Table 2). This is in accordance with the geochemical data that indicate low
399 concentration of OM, high detrital inputs and flooding. After this period, an isolated
400 wetland-like system formed between c. 1758 and c. 1954 CE (Zone 2) as indicated by the
401 decrease in *A. ambigua* and the increase in *A. alpigena*, a species associated with low
402 waters levels in tropical freshwater lakes (Table 2). The prevalence of *S. pinnata* and the
403 presence of the aerophil *D. confervacea* further support a very shallow, wetland-like
404 environment (Table 2). The decline in flooding and detrital inputs suggests a disconnection
405 to the river.

406 Permanent modern lake conditions were established after c. 1967, with moderately water
407 acidic conditions (Zone 3) as indicated by the dominance of benthic/tychoplanktonic
408 rather than planktonic diatoms including *Stauroneis neohyalina*, *Sellaphora alastos*,
409 *Gomphoneis eriense* and *Encyonema minutum* var. *pseudogracilis*. The further isolation of
410 the wetland and its transition to a lake after the 1960s is further supported by a marked
411 decline in detrital inputs and flooding along with an increase in autochthonous
412 productivity (OM content) and water column oxygenation. A recent palaeolimnological
413 study by Salgado et al., (2020) in the Panama Canal (Panama) similarly found that detrital
414 inputs that characterised historical riverine-wetland conditions declined after the

415 construction of Gatun Dam, while sediment reductive conditions shifted towards a more
416 oxygenated environment in response to a macrophyte expansion with creation of Gatun
417 Lake. Increases in organic matter and reduction in coarse sediment material associated
418 with lake production after artificial damming, or as in our case, after the fluvial input
419 declined, have been similarly described in floodplain lakes in the Yangtze River (Zeng et al.,
420 2018; Liu et al., 2012).

421 The suggested long-term transition from river, to a wetland-like environment and to a lake
422 fits other ontological process of South American floodplain lakes (Fayó et al., 2018;
423 Amoros & Bornette, 2002). These commonly, originate from a natural cutting off the
424 meandering neck of a river (Gaiser & Rühland, 2010), likely assisted by pronounced shifts
425 in precipitation regimes and sediment load that alter connectivity (Amoros & Bornette,
426 2002). In Colombia, ENSO brings extreme dry periods and the change from a river-
427 dominated system to a wetland-like environment in La San Juana presumably correlates
428 with a strong El Niño phase reported around c. 1750 CE (Li et al., 2011). Such dry climatic
429 conditions would have promoted a disconnection of a meander from the main river
430 channel (Fayó et al., 2018). The increase in P since the lake formation along with the
431 observed low responses to other ENSO events such as the 1992 El Niño or the 2011 La
432 Niña suggests that the lake is gradually becoming more productive and hence, likely more
433 sensitive to local environmental factors, such as nutrient and sediment runoff, than to
434 hydro-climatic events.

435

436 *Barbacoas Lake*

437 Temporal changes in diatom communities in Barbacoas Lake were mostly related to
438 variations in their relative abundances rather than to a succession of species. The MFA
439 analysis suggests that these long-term ecological changes were related to different
440 periods of varying degree of connectivity to the main river: first, a riverine-wetland-like
441 environment followed by periods of extreme drought and high flooding from the main
442 river. For instance, between c. 1959-1986 CE, the high OM content coupled with the
443 dominance of *A. distans*, *A. alpigena*, *Pinnularia* spp., *Eunotia* spp., and *C. meneghiniana*,
444 indicates shallow, productive, and turbid water conditions (Table 2). These geochemical
445 and diatom associations have been similarly described as characteristic of a wetland phase
446 during the evolution of a floodplain lake in the Colorado River, Argentina (Fayó et. al
447 2018). Wetland areas today in Barbacoas Lake are composed of large mats of floating and
448 emergent macrophytes thus that the water is rich in humic substances and poor in oxygen
449 (dissolved oxygen < 3 ppm; Table 1); such wetland conditions would have provided
450 suitable habitats for the dominant aerophil *D. confervacea* at 1960-1980 CE.

451 According to the MFA analysis, the lake and its connectivity to the Magdalena River have
452 been sensitive to extreme drier and wetter events post-1980. Extreme drought between
453 1989-1992 (Zone 2) inferred from the diatom composition, and confirmed by SPEI,
454 resulted in the reduction to almost a quarter of its original surface water area. This dry
455 spell concurs with the strong El Niño from 1992 that caused the partial desiccation of most
456 shallow water bodies in the country (Pestana Calderín & Mejía Arroyo, 2011). Drier

457 conditions not only would have diminished the lake-river connectivity, promoting
458 disconnection from the Magdalena river, but also must have increased evaporation rates
459 resulting in the partial desiccation of littoral areas; a process that regularly occurs during
460 the dry season across the lakes in the study area (personal observation by Lopera L &
461 Salgado J). In such smaller surface area lake with greater exposed littoral areas, aerophil
462 species such as *L. mutica* and *D. confervacea*, would have thrived (Table 2). Once the
463 intense ENSO dry climatic conditions ceased, the direct connection to the Magdalena River
464 is suggested to would have been re-established and the lake recovered its original surface
465 area. In 2011 the country experienced one of the greatest La Niña events of the last
466 century, where most of the Magdalena River catchment experienced unforeseen floods
467 (Euscategui & Hurtado, 2011). Our record shows that at the time, diatom counts were
468 barely legible in the fossil record while sedimentation rates increased significantly. Such
469 large increases in river sediment inputs would have affected diatom preservation and/or
470 dilute the diatom concentrations (Salgado et al., 2020; Reed, 1998).

471 *Ecological interpretation*

472 How aquatic communities are organised and respond to climatic or human-derived
473 stressors in tropical floodplain lakes largely depends on the degree and magnitude of the
474 disturbance, and on the spatial arrangement of lakes within the main hydrological
475 network (Erös, Olden, Schick, Schmera, & Fortin, 2012; Grant, Lowe, & Fagan, 2007).
476 Connected lakes for instance, are more dependent on the hydrological dynamics of the
477 main river, and hence that their aquatic communities often show a greater diversity and

478 low species turnover (through frequent organisms recruitment) than in isolated lakes
479 (Salgado et al., 2019; Swan & Brown, 2011). Isolated lakes on the other hand are likely to
480 present fewer organisms recruitment events, and thus local environmental factors such as
481 nutrient inputs (eutrophication) are likely to control community structure through
482 temporal species turnover (Salgado et al., 2019; Swan & Brown, 2011). Our
483 reconstructions are in general agreement with this framework of river metacommunities.
484 Since the establishment of modern conditions, the San Juana Lake has been less
485 dependent on the hydro-climatic variations, and thus less vulnerable to inter-annual
486 climate variability. As discussed, the extreme events of 1992 and 2011 did not greatly
487 affect the lake's surface area or its physical-chemical conditions. However, the marked
488 temporal successional trend in diatom species and the more recent (post 1960s) increases
489 in diatom species associated with productive environments (*Nitzschia spp.*, *C. cuspidata*
490 and *G. erriense*; Table 2), coupled with gradual increases in P, OM and sedimentation rates,
491 all indicates greater importance of in-lake factors in driving the diatom communities. The
492 more enclosed nature of the San Juana Lake may therefore facilitate a quicker response to
493 localised stressors such as changes in land use e.g. deforestation, and nutrient runoff from
494 agriculture and husbandry (Salgado et al., 2019; Bennion, Fluin & Simpson, 2004). In the
495 more connected Barbacoas Lake, diatom turnover was relatively low while diversity and
496 sediment yield were generally higher than those found at the more isolated San Juana
497 Lake. We also found that this lake is prone to be more affected by hydroclimatic events
498 such as ENSO than the San Juana Lake. In 1992 the diatom species composition (aerophil

499 *D. confervacea* and *L. mutica*) indicates a reduction in the water level of the lake; also
500 confirmed by the SPEI analysis.

501 During the last four decades, the Magdalena River basin has witnessed unprecedented
502 transformations in land cover (Restrepo et al., 2018; Suescún et al., 2017; Etter et al.,
503 2006). Forest clearance has greatly promoted erosion, increasing sediment loads and
504 nutrients into the Magdalena River (Restrepo et al., 2018). The latter likely promoting
505 eutrophication in associated water bodies (Suescún et al., 2017). Both of our study lakes
506 have recorded these marked increases in sedimentation, and suggests that land use
507 change and higher erosion is among one of the main drivers of anthropogenic stress in
508 these lakes. Connected lakes (in this case Barbacoas) in particular, seem to be more
509 susceptible to these increases in sedimentation rates.

510 **4.2 Palaeoflood interpretation**

511 Overall, we were able to discern the level of connectivity and river influence on the lakes
512 through the Zr/Fe ratio (a proxy for flooding). During dry years (SPEI values <0), the Zr/Fe
513 ratio was high; this could be explained by the droughts: coarser littoral sediments are
514 exposed during low water stands are reflected on coarser materials being transported
515 (Schillereff et al., 2014). As seen in Barbacoas Lake, the increasing river influence is
516 reflected by a decrease in OM being deposited by the river and by an increase in detrital
517 inputs (Rapuc et al., 2019); an opposite trend to what was observed in the San Juana Lake
518 since its formation. In accordance, the proxy for detrital inputs (Ti/Ca) showed a similar
519 behaviour to as the Zr/Fe ratio, while the opposite was observed for OM content. It is

520 expected that with a lower river influence, the OM in the systems increase through in-lake
521 primary productivity (Schillereff et al., 2014). These trend in the geochemical ratios allow
522 us to infer flood magnitudes and river connectivity with confidence, as it is consistent and
523 in accordance with the diatom interpretation.

524 **5. Concluding remarks**

525 In regards to our questions, 1 and 2, we show that these two lakes have had a very
526 different ontological histories controlled by the degree of connectivity to the Magdalena
527 River, and that this connectivity makes the more connected lake (Barbacoas) far more
528 sensitive to ENSO events than the more isolated lake San Juana, which in turn is far more
529 sensitive to local changes in the watershed. Future climate change scenarios suggest that
530 drier conditions will prevail in our study area (IDEAM, 2017). As indicated here, drier
531 conditions for the more isolated lakes, will likely increase water retention times and
532 promote in-lake productivity generating cascade effects such as anoxia and eutrophication
533 (Chislock et al., 2013). The degradation of these smaller and more isolated lakes is of great
534 concern. These lakes play key roles in water regulation and in offering temporal refuge for
535 the aquatic biota including endangered large mammals such as the river otter (*Lontra*
536 *longicauda*) and the American manatee (*T. manatus*; WCS Colombia, 2015), and key
537 economic species such as the Magdalena catfish (*P. magdaleniatum*) or the Bocachico (*P.*
538 *magdalenae*). As observed in Barbacoas, drier climates will inevitably lead to reductions in
539 lake size which will diminish habitats and the hydrologic regulatory capacity of these lakes
540 (Amoros & Bornette, 2002). These processes will likely have a positive feedback as more

541 sediment will be accumulated allowing for emergent plants to colonize newly formed
542 habitats which in turn, will promote the lake disconnection (Amoros & Bornette, 2002).
543 This, with the added concern of the increased sedimentation rates will put the lake at risk
544 of rapid clogging, and disappearance.

545 **ACKNOWLEDGEMENTS**

546 We thank the Palynology and Paleoecology Research Laboratory at University of Los
547 Andes for supporting Laura Lopera under her undergraduate thesis. We thank the
548 Government of Canada for supporting Laura's project under the Emerging Leaders in The
549 Americas (ELAP) scholarship. Fieldwork was supported by Fundación Proyecto Primates
550 and the research project "Efectos Antrópicos en Lagos Neotropicales" led by Jorge Salgado
551 through the postdoc fellowship "Es Tiempo de Volver" – Ministerio de Ciencia, Tecnología
552 e Innovación (MINCIENCIAS) and Los Andes University. We thank the Departments of
553 Geosciences and Chemistry at Universidad de Los Andes for XRF and LOI analysis
554 laboratory support. We also thank Fundación Proyecto Primates for logistic support on
555 fieldwork, hospitality and providing accessibility to the study area. The collections of
556 sediment material was assessed under the Permiso Marco de Recolección de Especímenes
557 Silvestres de La Biodiversidad Biológica con fines de Investigación Científica No Comercial
558 No. 1177 del 09 de octubre de 2014-IBD 0359. Collected lake sediment material was
559 transported to Los Andes University laboratories under the ANLA permit 2016004245-1-
560 000.

561

562 **CONFLICT OF INTEREST STATEMENT**

563 We declare no conflict of interest regarding patent or stock ownership, membership of a
564 company board of directors, membership of an advisory board or committee for a
565 company, and consultancy for or receipt of speaker's fees from a company.

566 **AUTHORS CONTRIBUTION:** J.S. conceived the ideas; J.S., and A.L., collected the sediment
567 cores; L.L., and J.S., collected the limnological data; L.L., and M.I.V., analysed the diatom
568 data and L.L., analysed the XRF data. L.L., and J.S., performed statistical analysis and L.L.,
569 wrote the first manuscript; J.S., M.I.V., C.G., and A.L., contributed essentially to the
570 interpretation and wording of the final version.

571 **DATA AVAILABILITY**

572 Should the manuscript be accepted, the data supporting the results will be archived in an
573 appropriate public repository (Dryad, Figshare or Hal) and the data DOI will be included at
574 the end of the article.

575 **REFERENCES**

576 Angarita, H., Wickel, A. J., Sieber, J., Chavarro, J., Maldonado-Ocampo, J. A., Herrera-R,
577 G. A., ... & Purkey, D. (2018). Basin-scale impacts of hydropower development on the
578 Mompós Depression wetlands, Colombia. *Hydrology and Earth System Sciences*, 22, 28-
579 39.

580 Angel-Escobar, D. C., Rodríguez-Buriticá, S., Buitrago-Grisales, M. C. (2014). *Sustento*
581 *para la declaratoria de un área protegida pública en las ciénagas de Barbacoas, Municipio*
582 *de Yondó, Antioquia*. (1st ed.) Fundación Biodiversa, Colombia.

583 Amoros, C., & Bornette, G. (2002). Connectivity and biocomplexity in waterbodies of
584 riverine floodplains. *Freshwater biology*, 47, 761–776.

585 Appleby, P. G., Birks, H. H., Flower, R. J., Rose, N., Peglar, S. M., Ramdani, M., ... &
586 Fathi, A.A. (2001). Radiometrically determined dates and sedimentation rates for recent
587 sediments in nine North African wetland lakes (the CASSARINA Project). *Aquatic*
588 *Ecology*, 35, 347–367.

589 Ayram, C. A. C., Rothlisberger, A. E., Timote, J. J. D., Buritica, S. R., Ramirez, W., &
590 Corzo, G. (2020). Spatiotemporal Evaluation of The Human Footprint in Colombia: Four
591 Decades of Anthropogenic Impact in Highly Biodiverse Ecosystems. *Ecological Indicators*. Doi:
592 10.1016/j.ecolind.2020.106630

593 Bahls, L. (2010) *Stauroneis* in the Northern Rockies: 50 species of *Stauroneis* sensu
594 stricto from western Montana, northern Idaho, northeastern Washington and
595 southwestern Alberta, including 16 species described as new. *Northwest Diatoms*, Volume
596 4.

597 Bahls, L. (2014). New diatoms from the American West-A tribute to citizen
598 science. *Proceedings of the Academy of Natural Sciences of Philadelphia*, 163, 61–84.

599 Battarbee, R. W. 1986. *Diatom analysis*. In: Berglund B. E. (ed.) Handbook of
600 Holocene palaeoecology and palaeohydrology. John Wiley and Sons, Chichester.

601 Bennion, H., Fluin, J., & Simpson, G. L. (2004). Assessing eutrophication and
602 reference conditions for Scottish freshwater lochs using subfossil diatoms. *Journal of*
603 *applied Ecology*, 41, 124–138.

604 Best, J. (2019). Anthropogenic stresses on the world’s big rivers. *Nature*
605 *Geoscience*, 12(1), 7-21.

606 Bicudo, D. C., Tremarin, P. I., Almeida, P. D., Zorzal-Almeida, S., Wengrat, S.,
607 Faustino, S. B., ... & Morales, E. A. (2016). Ecology and distribution of *Aulacoseira*
608 species (Bacillariophyta) in tropical reservoirs from Brazil. *Diatom Research*, 31, 199–
609 215.

610 Bishop, I. W., Esposito, R. M., Tyree, M. and Spaulding, S. A. (2017). A diatom
611 voucher flora from selected southeast rivers (USA). *Phytotaxa*, 332, 101–140.

612 Bona, F., Falasco, E., Fassina, S., Griselli, B., & Badino, G. (2007). Characterization of
613 diatom assemblages in mid-altitude streams of NW Italy. *Hydrobiologia*, 583, 265–274.

614 Boyle, J. F. (2002). *Inorganic geochemical methods in palaeolimnology*. In Tracking
615 environmental change using lake sediments (pp. 83-141). Springer, Dordrecht.

616 Bradbury, J. P., & Van Metre, P. C. (1997). A land-use and water-quality history of
617 White Rock Lake reservoir, Dallas, Texas, based on paleolimnological analyses. *Journal*
618 *of Paleolimnology*, 17, 227–227.

619 Edlund, M. B., Burge, R. L. and Spaulding, S. A. (2017) The transfer of *Navicula*
620 *cuspidata var. obtusa* to *Craticula* (Bacillariophyceae). *Notulae Algarum*, 19.

621 Burge, D. R., Edlund, M. B., & Frisch, D. (2018). Paleolimnology and resurrection
622 ecology: The future of reconstructing the past. *Evolutionary Applications*, 11, 42–59.

623 Caballero, H. Durango, C. Giraldo, C. A. (2001). Los Humedales del Magdalena
624 Medio Antioqueño Desde Una Perspectiva Física y Sociocultural. *Gestión y Ambiente*,
625 4.

626 Cantonati, M., Kelly, M. G., & Lange-Bertalot, H. (2017). *Freshwater benthic*
627 *diatoms of Central Europe: over 800 common species used in ecological*
628 *assessment*. English edition with update taxonomy and added species. Schmitt-
629 Oberreifenberg: Koeltz Botanical Books, 1–942.

630 Carvajal–Quintero, J. D., Januchowski–Hartley, S. R., Maldonado–Ocampo, J. A.,
631 Jézéquel, C., Delgado, J., & Tedesco, P. A. (2017). Damming fragments species' ranges
632 and heightens extinction risk. *Conservation Letters*, 10, 708–716.

633 Chislock, M. F., Doster, E., Zitomer, R. A., & Wilson, A. E. (2013). Eutrophication:
634 causes, consequences, and controls in aquatic ecosystems. *Nature Education*
635 *Knowledge*, 4, 10.

636 Cohen, A. S. (2003). *Paleolimnology: the history and evolution of lake systems*.
637 Oxford University Press, New York.

638 Collins, S. L., Micheli, F. & Hartt, L. (2000). A method to determine rates and
639 patterns of variability in ecological communities. *Oikos*, 91, 285–293.

640 Collins, S. L., Suding, K. N., Cleland, E. E., Batty, M., Pennings, S. C., Gross, K. L.
641 (2008). Rank clocks and plant community dynamics. *Ecology*, 89, 3534–3541.

642 Conrey, R. M., Goodman-Elgar, M., Bettencourt, N., Seyfarth, A., Van Hoose, A., &
643 Wolff, J. A. (2014). Calibration of a portable X-ray fluorescence spectrometer in the
644 analysis of archaeological samples using influence coefficients. *Geochemistry:
645 Exploration, Environment, Analysis*, 14, 291–301.

646 Dean, W. E. (1974). Determination of carbonate and organic matter in calcareous
647 sediments and sedimentary rocks by loss on ignition; comparison with other
648 methods. *Journal of Sedimentary Research*, 44, 242–248.

649 Death, R. G. (2010). Disturbance and Riverine Benthic Communities: what has it
650 contributed to general ecological theory? *River Research and Applications*, 26, 15–25.

651 Davies, S. J., Lamb, H. F., & Roberts, S. J. (2015). *Micro-XRF core scanning in
652 palaeolimnology: recent developments*. In *Micro-XRF studies of sediment cores*.
653 Springer, Dordrecht.

654 Ekdahl, E. J., Teranes, J. L., Guilderson, T. P., Turton, C. L., McAndrews, J. H.,
655 Wittkop, C. A., & Stoermer, E. F. (2004). Prehistorical record of cultural eutrophication
656 from Crawford Lake, Canada. *Geology*, 32, 745–748.

657 Erős, T., Olden, J. D., Schick, R. S., Schmera, D., & Fortin, M. J. (2012).
658 Characterizing connectivity relationships in freshwaters using patch-based
659 graphs. *Landscape ecology*, 27, 303–317.

660 Etter, A., C. McAlpine, D. Pullar & H. Possingham. (2006). Modelling the conversion
661 of Colombian lowland ecosystems. *Journal of Environmental Management*, 79, 74–87.

662 Euscategui, C., & Hurtado, G. (2011). Análisis del Impacto Del Fenómeno “La Niña”
663 2010-2011 En La Hidroclimatología Del País. Instituto de Ambiente y desarrollo-
664 IDEAM.

665 Fayó, R., Espinosa, M. A., Vélez-Agudelo, C. A., Pan, J., & Isla, F. I. (2018). Diatom-
666 based reconstruction of Holocene hydrological changes along the Colorado River
667 floodplain (northern Patagonia, Argentina). *Journal of Paleolimnology*, 60, 427–443.

668 Gaiser, E., & Rühland, K. (2010). Diatoms as indicators of environmental change in
669 wetlands and peatlands. *The diatoms: applications for the environmental and earth*
670 *sciences*, (2nd Ed.), 473–496.

671 Gasdia-Cocharne, M. (2017) XRF Glossary: Common Analysis Techniques Explained.

672 Gell P, Baldwin D, Little F, Tibby J, Hancock G. 2007. The impact of regulation and
673 salinisation on floodplain lakes: the lower River Murray, Australia. *Hydrobiologia*, 591,
674 135–146.

675 Grant, C., E. H., Lowe, W. H., & Fagan, W. F. (2007). Living in the branches:
676 population dynamics and ecological processes in dendritic networks. *Ecology*
677 *letters*, 10, 165–175.

678 Hallett, L. M., Jones, S. K., MacDonald, A. A. M., Jones, M. B., Flynn, D. F.,
679 Ripplinger, J., ... & Collins, S. L. (2016). codyn: an R package of community dynamics
680 metrics. *Methods in Ecology and Evolution*, 7, 1146–1151.

681 Hernández-Atilano, E., Aguirre, N. J., Palacio, J. A., & Ramírez-Restrepo, J. J. (2008).
682 Variación espacio-temporal de la asociación fitoplanctónica en diferentes momentos
683 del pulso hidrológico en la ciénaga del Ayapel (Córdoba), Colombia. *Actualidades*
684 *Biológicas*, 30, 67–81.

685 Instituto de Ambiente y desarrollo –IDEAM. (2017). Análisis de Vulnerabilidad y
686 Riesgo por Cambio Climático en Colombia. Tercera Comunicación Nacional de
687 Colombia a la Convención de las Naciones Unidas Sobre Cambio Climático (CMNUCC).
688 Bogotá.

689 Juggins, S. (2009). Rioja: Analysis of Quaternary Science Data. R package version
690 0.5–6. Available online at: <http://cran.r-project.org/package=rioja>

691 Junk, W. J., Bayley, P. B., & Sparks, R. E. (1989). The flood pulse concept in river-
692 floodplain systems. *Canadian special publication of fisheries and aquatic sciences*, 106,
693 110–127.

694 Kulichová, J., & Fialová, M. (2016). Correspondence between morphology and
695 ecology: morphological variation of the *Frustulia crassinervia-saxonica* species
696 complex (bacillariophyta) reflects the ombro-minerotrophic gradient. *Cryptogamie,*
697 *Algologie*, 37, 15–29.

698 Kociolek, J.P. and Stoermer, E.F. (1988) Taxonomy, ultrastructure and distribution
699 of *Gomphoneis herculeana*, *G. eriense* and closely related species (Naviculales:
700 Gomphonemataceae). *Proceedings of the Academy of Natural Sciences of Philadelphia*,
701 140, 24–97.

702 Krammer, K & Lange-Bertalot, H. (1986). Bacillariophyceae 1 Teil: Naviculaceae.
703 Jena: VEB Gustav Fisher.

704 Krammer, K & Lange-Bertalot, H. (1991a). Bacillariophyceae. 3 Teil: Centrales,
705 Fragilariaceae, Eunotiaceae, Achnanthaceae. Jena:VEB Gustav Fisher.

706 Krammer, K & Lange-Bertalot, H. (1991b). Bacillariophyceae. 4 Teil:
707 Achnanthaceae, Kritische Ergänzungen zu *Navicula* (Lineolatae) und *Gomphonema*.
708 Jena: VEB Gustav Fisher.

709 La Hée, J. M., & Gaiser, E. E. (2012). Benthic diatom assemblages as indicators of
710 water quality in the Everglades and three tropical karstic wetlands. *Freshwater*
711 *Science*, 31, 205–221.

712 Lake, P. S. (2000). Disturbance, patchiness, and diversity in streams. *Journal of the*
713 *north american Benthological society*, 19, 573–592.

714 Lange-Bertalot, H., & Metzeltin, D. (2007). Tropical Diatoms of South America I.
715 ARG Gantner.

716 Li, J., Xie, S. P., Cook, E. R., Huang, G., D'arrigo, R., Liu, F., ... & Zheng, X. T. (2011).
717 Interdecadal modulation of El Niño amplitude during the past millennium. *Nature*
718 *Climate Change*, 1, 114.

719 Liu, B., Williams, D. M., Blanco, S., & Jiang, X. (2017). Two new species of *Luticola*
720 (Bacillariophyta) from the Wuling Mountains Area, China. *Nova Hedwigia*, 146, 197–
721 208.

722 Liu, Q., Yang, X., Anderson, N. J., Liu, E., & Dong, X. (2012). Diatom ecological
723 response to altered hydrological forcing of a shallow lake on the Yangtze floodplain, SE
724 China. *Ecohydrology*, 5, 316–325.

725 Loganathan, P., Pruhanteen, A., Humane, S. K., & Hussain, S. M. (2014).
726 Distribution of Freshwater Diatoms in the Sediments of the Perumal Lake, Cuddalore
727 District, Tamil Nadu. *Gondwana Geological Magazine*, 15, 79–84. _

728 Lowe, R., Kheiri, S. (2015). *Cyclotella meneghiniana*. In *Diatoms of North America*.
729 Retrieved November 29, 2019, from
730 https://diatoms.org/species/cyclotella_meneghiniana

731 Metzeltin, D., & Lange-Bertalot, H. (1998). *Tropical diatoms of South America I:*
732 *Iconographia Diatomologica*. Koeltz, Stuttgart.

733 Mojica, J. I., Galvis, G., Sánchez-Duarte, P., Castellanos, C., & Villa-Navarro, F. A.
734 (2006). Peces del valle medio del río Magdalena, Colombia. *Biota colombiana*, 7.

735 Montoya Moreno, Y., & Aguirre, N. (2009). Estado del arte de la limnología de lagos
736 de planos inundables (Ciénagas) en Colombia. *Gestión y ambiente*, 12.

737 Oksanen, J., Blanchet, F. G., Kindt, R., Legendre, P., O'hara, R. B., Simpson, G. L., ...
738 & Wagner, H. (2010). *Vegan: community ecology package*. R package version 1.17-4.

739 Pagès, J. 2002. "Analyse Factorielle Multiple Appliquée Aux Variables Qualitatives
740 et Aux Données Mixtes." *Revue Statistique Appliquée*, 4, 5-37.

741 Pestana Calderín, M. C., & Mejía Arroyo, D. C. (2011) *La gran evolución energética*
742 *en Colombia*. PhD Thesis, Universidad del Rosario.

743 Poff, N. L., & Ward, J. V. (1989). Implications of streamflow variability and
744 predictability for lotic community structure: a regional analysis of streamflow
745 patterns. *Canadian journal of fisheries and aquatic sciences*, 46, 1805-1818.

746 Poulíčková, A., Špačková, J., Kelly, M. G., Duchoslav, M., & Mann, D. G. (2008).
747 Ecological variation within Sellaphora species complexes (Bacillariophyceae):
748 specialists or generalists?. *Hydrobiologia*, 614, 373–386.

749 Ramirez, A. M., & Plata-Diaz, (2008). Diatomeas perifíticas en diferentes tramos de
750 dos sistemas lóticos de alta montaña (Páramo de Santurbán, Norte de Santander,
751 Colombia) y su relación con las variables ambientales. *Acta Biológica Colombiana*, 13,
752 199–215.

753 Rapuc, W., Sabatier, P., Arnaud, F., Palumbo, A., Develle, A. L., Reyss, J. L., ... &
754 Dumoulin, J. P. (2019). Holocene-long record of flood frequency in the Southern Alps
755 (Lake Iseo, Italy) under human and climate forcing. *Global and planetary change*, 175,
756 160–172.

757 Raupp, S. V., Torgan, L. C., & Melo, S. (2009). Planktonic diatom composition and
758 abundance in the Amazonian floodplain Cutiaú Lake are driven by the flood pulse.
759 *Acta Limnologica Brasiliensia*, 21, 227–234.

760 Reed, J. M. (1998). Diatom preservation in the recent sediment record of Spanish
761 saline lakes: implications for palaeoclimate study. *Journal of Paleolimnology*, 19, 129–
762 137.

763 Resh, V. H., Brown, A. V., Covich, A. P., Gurtz, M. E., Li, H. W., Minshall, G. W., ... &
764 Wissmar, R. C. (1988). The role of disturbance in stream ecology. *Journal of the North
765 American benthological society*, 7, 433–455.

766 Restrepo, J. (2015). El impacto de la deforestación en la erosión de la cuenca del río
767 Magdalena (1980-2010). *Revista de la Academia Colombiana de Ciencias Exactas,*
768 *Físicas y Naturales*, 39, 250–267.

769 Restrepo, J. D., & Escobar, H. A. (2018). Sediment load trends in the Magdalena
770 River basin (1980–2010): Anthropogenic and climate-induced
771 causes. *Geomorphology*, 302, 76–91.

772 Salgado, J., Sayer, C. D., Brooks, S. J., Davidson, T. A., Baker, A. G., Willby, N., ... &
773 Okamura, B. (2019). Connectivity and zebra mussel invasion offer short-term buffering
774 of eutrophication impacts on floodplain lake landscape biodiversity. *Diversity and*
775 *Distributions*, 25, 1334–1347.

776 Salgado, J., Vélez, M. I., González-Arango, C., Rose, N. L., Yang, H., Huguet, C., ... &
777 O'Dea, A. (2020). A century of limnological evolution and interactive threats in the
778 Panama Canal: Long-term assessments from a shallow basin. *Science of The Total*
779 *Environment*, 729.

780 Schillereff, D. N., Chiverrell, R. C., Macdonald, N., & Hooke, J. M. (2014). Flood
781 stratigraphies in lake sediments: A review. *Earth-Science Reviews*, 135, 17–37.

782 Suescún, D., Villegas, J. C., León, J. D., Flórez, C. P., García-Leoz, V., & Correa-
783 Londono, G. A. (2017). Vegetation cover and rainfall seasonality impact nutrient loss
784 via runoff and erosion in the Colombian Andes. *Regional Environmental Change*, 17,
785 827–839.

786 Swan, C. M., & Brown, B. L. (2011). Advancing theory of community assembly in
787 spatially structured environments: local vs regional processes in river
788 networks. *Journal of the North American Benthological Society*, 30, 232–234.

789 Tjallingii, R., Rohl, U., Kolling, M., Bickert, T. (2007). Influence of the water content
790 on X-ray fluorescence core scanning measurements in soft marine sediments.
791 *Geochemistry Geophysics Geosystems* 8, 1–12.

792 Tockner, K., Pusch, M., Borchardt, D., & Lorang, M. S. (2010). Multiple stressors in
793 coupled river–floodplain ecosystems. *Freshwater Biology*, 55, 135–151.

794 Tuji, A. (2015). Distribution and taxonomy of the *Aulacoseira distans* species
795 complex found in Japanese harmonic artificial reservoirs. *Bulletin of the National
796 Museum of Nature and Science Series B (Botany)*, 41, 53–60.

797 Van Looy, K., Tonkin, J. D., Flourey, M., Leigh, C., Soininen, J., Larsen, S., ... & Datry,
798 T. (2019). The three Rs of river ecosystem resilience: Resources, recruitment, and
799 refugia. *River Research and Applications*, 35, 107–120.

800 Vélez, M. I., Hooghiemstra, H., & Metcalfe, S. (2005). Fossil and modern diatom
801 assemblages from the savanna lake El Piñal, Colombia: an environmental
802 reconstruction. *Diatom Research*, 20, 387–407.

803 Vicente-Serrano, S. M., Beguería, S., & López-Moreno, J. I. (2010). A multiscalar
804 drought index sensitive to global warming: the standardised precipitation
805 evapotranspiration index. *Journal of climate*, 23, 1696–1718.

806 Viktória, B., Török, P., Kókai, Z., Lukács, Á., Enikő, T., Tóthmérész, B., & Bácsi, I.
807 (2017). Ecological background of diatom functional groups: Comparability of
808 classification systems. *Ecological Indicators*, 82,183–188.

809 Wild Conservation Society–WCS Colombia (2015). Confirman presencia del Manatí
810 del Caribe en ciénagas de Cimitarra (Santander).

811 Wood, S., & Wood, M. S. (2015). Package ‘mgcv’. R package version, 1, 29.

812 Zeng, L., McGowan, S., Cao, Y., & Chen, X. (2018). Effects of dam construction and
813 increasing pollutants on the ecohydrological evolution of a shallow freshwater lake in
814 the Yangtze floodplain. *Science of the Total Environment*, 621, 219–227.

815

816 **FIGURE CAPTIONS**

817 **FIGURE 1** (A) map of Colombia showing the locations of the Magdalena River and the
818 study area (red square); (B) zoom into Barbacoas Lake and San Juana Lake showing the
819 coring locations of LBARB1 core (red circle) and LSAN1 core (red star) respectively; (C)
820 example of littoral areas in the lakes during the dry season.

821 **FIGURE 2** Radiometric chronology of the cores (a) LSAN1 (San Juana Lake) and (b) LBARB1
822 (Barbacoas Lake), showing the CRS model ^{210}Pb dates (solid line) and sedimentation rates
823 (dash blue line). Black dash line in (a) indicates the modelled age beyond the ^{210}Pb dates,
824 through lineal regression analysis assuming a constant sedimentation rate of 0.087 cm yr^{-1}
825 that corresponds to the mean value of the last four adjacent dated sediment samples.

826 **FIGURE 3** (a) Stratigraphy of diatoms assemblages found in the sediment record of the
827 LSAN1 core (San Juana Lake); and (b) Results of Rank Clock Analysis (RCA) on diatoms
828 assemblages of LSAN1 core. RCA identifies which species show the greatest change in
829 abundance (i.e. those distancing from the centre of the diagram) at temporal zones of
830 change revealed by clustering analysis on a clock-like diagram, where 12 o'clock on the
831 vertical axis is the starting point of the data.

832 **FIGURE 4** (a) Stratigraphy of diatoms assemblages found in the sediment record of the
833 LBARB1 core (Barbacoas Lake); and (b) Results of Rank Clock Analysis (RCA) on diatoms
834 assemblages of LBARB1 core. RCA identifies which species show the greatest change in
835 abundance (i.e. those distancing from the centre of the diagram) at temporal zones of

836 change revealed by clustering analysis on a clock-like diagram, where 12 o'clock on the
837 vertical axis is the starting point of the data.

838 **FIGURE 5** Surface area (km²) of the two study lakes during the years 1985 (A; Barbacoas
839 Lake 8.7 Km²; San Juana Lake 0.64 Km²), 1992 (B; Barbacoas Lake 2.8 Km²; San Juana Lake
840 0.56 Km²), 2011 (C; Barbacoas Lake 8.4 Km²; San Juana Lake 0.59 Km²) and 2016 (D;
841 Barbacoas Lake 10.37 Km²; San Juana Lake 0.52 Km²).

842 **FIGURE 6** Generalised Additive Model (GAM) plots on temporal changes in organic matter
843 content (LOI), Mn/Fe ratios (proxy for oxygenation in the water column), Ti/Ca ratios
844 (proxy for detrital input), Zr/Fe ratios (proxy for flooding) and phosphorus concentrations
845 (proxy for increases in productivity) in the cores (a) LSAN1–San Juana Lake; (b) LBARB1–
846 Barbacoas Lake; and (c) GAM results on temporal Zr/Fe ratios and SPEI index data and in
847 LSAN1 and LBARB1 cores respectively.

848 **FIGURE 7** Multiple Factor Analysis (MFA) plots for the cores (a) LSAN1 and (b) LBARB1
849 showing the variation in diatoms functional groups (Plankton in green, Acidic/dystrophic
850 in yellow and Benthic/productive in grey), and selected geochemical ratios and elements
851 (purple) Fe/Mn, Ti/Ca, Zr/Fe and P, organic matter content (LOI) and sedimentation rates.
852 The contribution of each variable is indicated according to a colour scale, being red the
853 highest value and green the lowest. Black dash arrows indicate temporal trajectory of
854 sediment sample change. The contribution of each group at dimensions 1 and 2 are
855 indicated.

856

87
88

857 **Table 1.** Mean values of physical-chemical parameters measured in situ at the littoral and
 858 open water areas of the San Juana Lake and Barbacoas Lake during 2018.

Lake	Depth (m)	Secchi depth (m)	Temperature (°C)	pH	Dissolved oxygen/surface (ppm)	Dissolved oxygen/bottom (ppm)
<u>Barbacoas</u>						
Littoral	0.62	0.29 ±0.40	33.6 ±0.59	7.2 ±0.34	4.84 ±0.57	2.81 ±1.23
In-lake	1.5	0.49 ±0.54	33.6 ±0.35	7.3 ±0.18	5.11 ±0.64	2.34 ±1.45
<u>San Juana</u>						
Littoral	2.2	0.57 ±0.79	29.9 ±1.18	7.5	-	-
In-lake	2.4	0.5 ±0.31	30.4 ±0.68	7.2	-	-

859

860 **Table 2.** Diatom species recorded in the sediment record of the San Juana Lake and
 861 Barbacoas Lake. The ecology, associated functional group, reference and ecological
 862 preference suggested by our data is presented.

Species	Ecology	Functional group	Reference	Ecological interpretation in our study †
<i>Aulacoseira ambigua</i>	Preference for productive waters, water mixing and low light conditions.	Plankton	Bicudo <i>et al.</i> , 2016	Mixing conditions, increased turbidity
<i>Aulacoseira alpigena</i>	Mixing of the water column, adapted to low light conditions and low pH. Also associated with an increase in runoff. Found in 50 cm of water in the waters from a Paramo mire in Colombia (Velez, personal observation)	Plankton	Bradbury & Van Metre, 1997	Mixing conditions, increased turbidity
<i>Aulacoseira granulata</i>	Riverine species commonly found on floodplain	Plankton	Hernández-Atilano <i>et al.</i> , 2008	River influence/mixing conditions

	lakes. Common in flooding areas (floodplains); reported on similar floodplains in Ayapel, Colombia			
<i>Aulacoseira granulata</i> var. <i>angustissima</i>	Eutrophic lakes and rivers	Plankton	Bicudo <i>et al.</i> , 2016	River influence/mixing conditions
<i>Aulacoseira herzogii</i>	Mesotrophic to eutrophic lakes; Slightly acidic waters.	Plankton	Bicudo <i>et al.</i> , 2016 Velez, 2005	River influence/mixing conditions/higher turbidity nutrients
<i>Aulacoseira distans</i>	Turbid freshwater. Alkaline and eutrophic ecosystems.	Plankton	Tuji, 2015	River influence/mixing conditions
<i>Cyclotella meneghiniana</i>	Shallow, nutrient rich waters.	Plankton	Lowe & Kheiri, 2015	River influence/higher turbidity
<i>Fragilaria</i>	Mesotrophic to eutrophic lakes	Plankton	Ekdahl, Teranes, Guilderson, Turton, McAndrews, Wittkop, & Stoermer, 2004	
<i>Diadsmis confervacea</i>	Aerophil, Shallow still water	Aerophil	Raupp, S. V., Torgan, L. C., & Melo, S. (2009)	In-Lake conditions

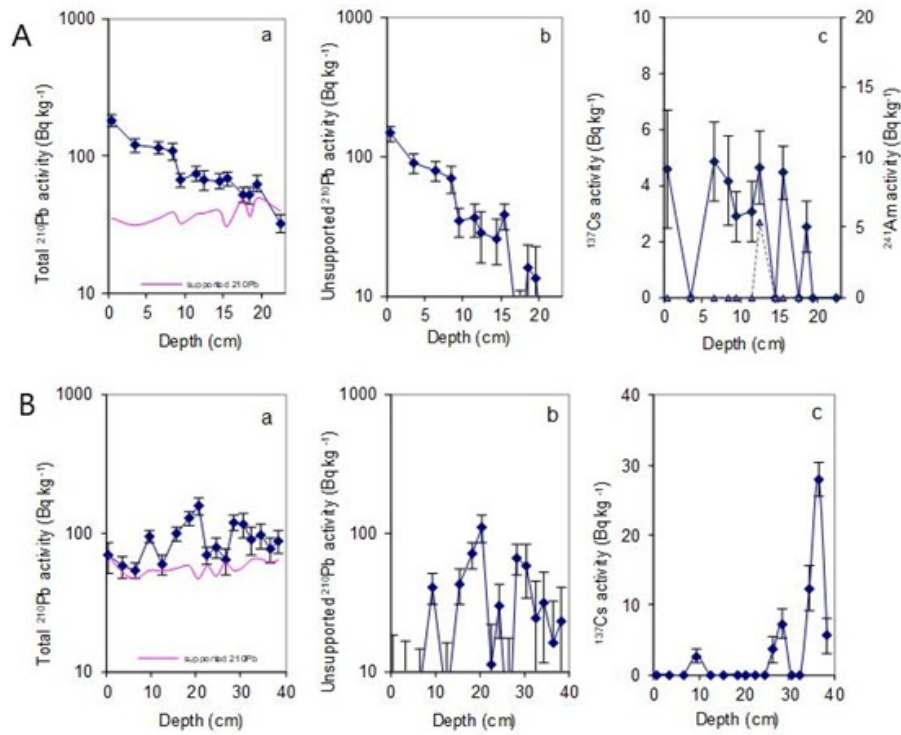
<i>Staurosira pinnata</i>	Shallow water and high quality indicator, high tolerance to dissolved inorganic carbon	Aerophil	Bona <i>et al.</i> , 2007	Shallow waters
<i>Luticola mutica</i>	Mosses, stones, wet walls and exposed soil	Aerophil	Liu <i>et al.</i> , 2017	Shallow waters/exposed soil
<i>Encyonema minutum</i>	Freshwater species commonly found on weakly acidic environments.	Benthic (Dystrophic)	Bishop <i>et al.</i> , 2017	In-lake/dystrophic
<i>Eunotia</i>	Low pH conditions	Benthic (Dystrophic)	La Heé & Gaiser, 2012	In-lake/dystrophic
<i>Gomphonema augur</i>	Lakes with moderately acidic pH; reported on the Amazon floodplains	Benthic (Dystrophic)	Metzeltin & Lange-Bertalot, 1998	
<i>Neidium saccoense</i>	Low pH conditions; Abundant in wetlands	Benthic (Dystrophic)	Burge <i>et al.</i> , 2017	Shallow waters/marsh
<i>Pinnularia</i>	Low pH conditions; lakes and wet soil	Benthic (Dystrophic)	La Heé & Gaiser, 2012	In-lake/dystrophic

<i>Placoneis cf. tersa</i>	Shallow, low alkalinity and meso-eutrophic lakes	Benthic (Dystrophic)	Pouličková, Špačková, Kelly, Duchoslav, & Mann, (2008)	
<i>Sellaphora alastos</i>	Ponds and small lakes, oligo-dystrophic environments	Benthic (Dystrophic)	Bahls, 2014	
<i>Sellaphora laevisissima</i>	Lakes and rivers, mildly acidic environments	Benthic (Dystrophic)	Burge, Edlund & Spaulding, 2017	
<i>Stauroneis fluminopsis</i>	Lakes and wetlands	Benthic (Dystrophic)	Bahls, 2010	
<i>Stauroneis neohyalina</i>	Preference for small humic-rich lakes and wetlands.	Benthic (Dystrophic)	Cantonati, M., Kelly, M. G., & Lange-Bertalot, H. (2017)	
<i>Fristulia crassinervia</i>	Oligotrophic habitats	Benthic (Dystrophic)	Kulichová & Fialová, 2016	
<i>Gomphoneis erienze</i>	Found on lakes; sensitive to human disturbance; tolerant to turbulence	Benthic (productive)	Kociolek & Stoermer, 1998	
<i>Nitzschia</i>	Tolerant to pollution and high dissolved carbon	Benthic (productive)	Ramírez & Plata-Díaz, 2008	
<i>Actinella disjuncta</i>	Environments rich in humic	Benthic (productive)	Lange-Bertalot &	Productivity/river influence

	acids. Bog flora.		Metzeltin,2007
<i>Hantzschia elongata</i>	Ponds and wetlands, eutrophication	Benthic (productive)	Loganathan, Pruhantheen, Humane & Hussain, 2014

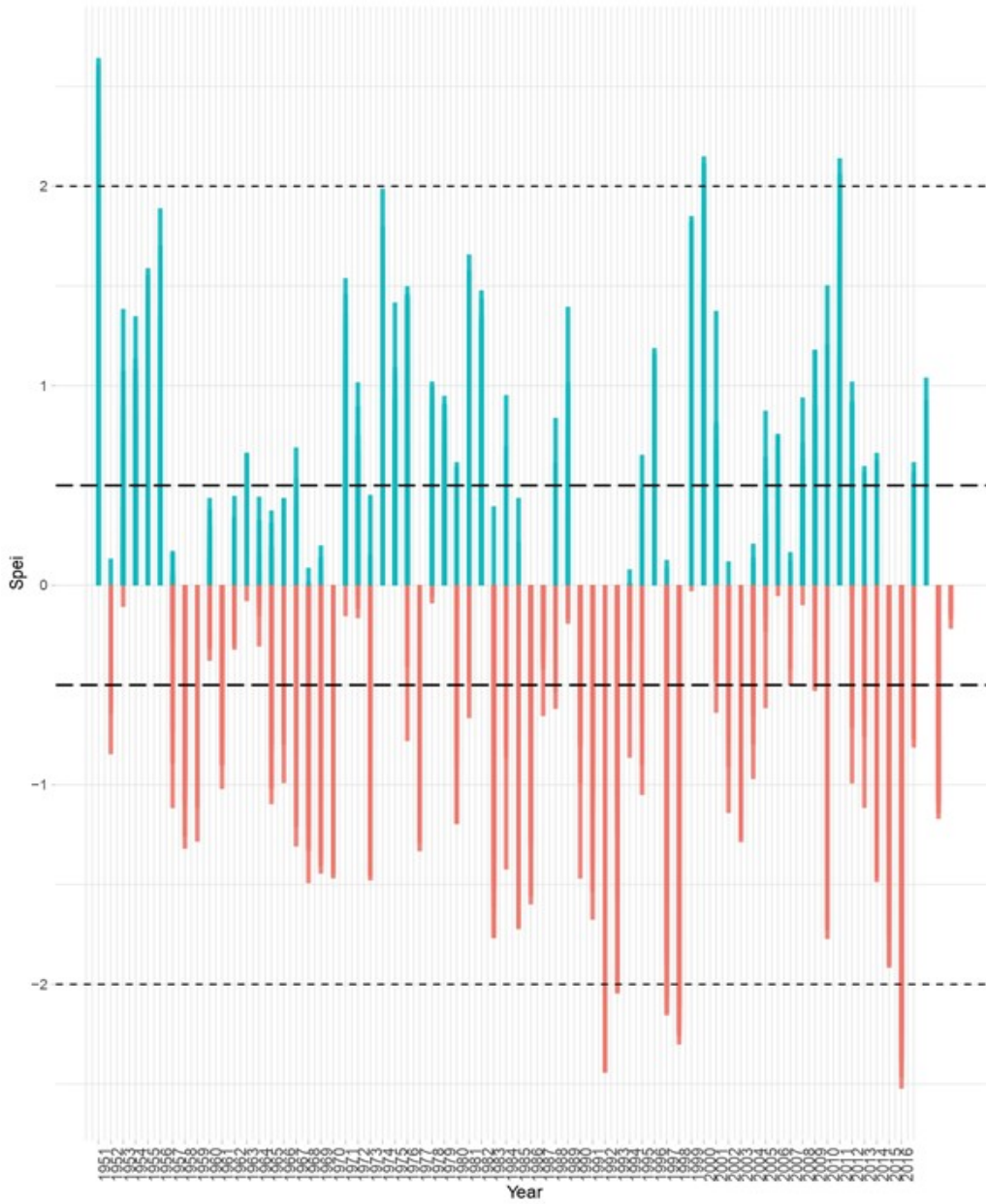
863 †The ecological interpretations of were done only for the most relevant species por the
864 paleo reconstruction of the lakes.

865



867

868 **Figure S1.** Fallout radionuclide concentrations in (A) core LSAN1 (San Juana Lake); and (B)
 869 LBARB1 (Barbacoas Lake), showing (a) total ^{210}Pb , (b) unsupported ^{210}Pb , and (c) ^{137}Cs and
 870 ^{241}Am concentrations versus depth.



871

872 **Figure S2.** SPEI analysis data for the identification of dry and wet years during 1959-2016.

873

874

875